Physics Letters A ••• (••••) •••–•••

Contents lists available at ScienceDirect

Physics Letters A

www.elsevier.com/locate/pla

First-principles predictions of the geometries and electronic structures of tungsten ditelluride nanoribbons

Jian-Hao Wang [a], Wei Yang [b], Mei Zhou [c], Yu Yang [c,*], Jie-Yun Yan [b,*], Ping Zhang [c]

[a] School of Science, Beijing University of Posts and Telecommunications, Beijing 100876, China
[b] Beijing University of Posts and Telecommunications, Beijing 100876, China
[c] Institute of Applied Physics and Computational Mathematics, P.O. Box 8009, Beijing 100088, China

ARTICLE INFO

Article history:
Received 8 February 2018
Received in revised form 31 May 2018
Accepted 15 June 2018
Available online xxxx
Communicated by R. Wu

Keywords:
WTe_2 nanoribbons
Electronic structure

ABSTRACT

First-principles calculations are carried out to predict the structures and electronic properties of 2H- and Td-WTe_2 nanoribbons with different termination edges. It is found that the 2H-WTe_2 nanoribbon along the armchair direction and the Td-WTe_2 nanoribbon along the *X* direction show semiconducting characters with tunable band gaps. The 2H-WTe_2 nanoribbon along the zigzag direction and the Td-WTe_2 nanoribbon along the *Y* direction show metallic characters.

1. Introduction

Due to the quantum confinement on electron movements and unique folding Fermi level, one-dimensional materials such as nanorods, nanotubes, nanowires, and nanoribbons show interesting collective electron behaviors like various density waves and adjustable electronic properties [1]. These properties enrich one-dimensional materials with both fundamental importance and practical applications. One compelling example is graphene nanoribbons, showing lots of fantastic properties. For example, graphene nanoribbons have highly tunable energy band gaps [2,3], and robust edge states [4], and undergo transitions to half-metal after applying external electric biases [5]. Beyond graphene, transition metal dichalcogenides (TMD) emerge as another important class of two dimensional system with inherently interesting physical properties, such as quantum spin Hall effect, Weyl semimetallicity, superconductivity, and extremely large magnetoresistance, etc. [6–11]. When reduced from bulk to two-dimensional monolayers, and further from two-dimensional monolayers to one-dimensional nanoribbon geometries, the very compound nature of the TMD systems further introduces more complexities and singularities [12–19].

Among the TMD family, WTe_2 has attracted much attention recently, because it exhibits extremely large magnetoresistance [9,20], pressure-driven superconductivity [21,22], and type-II Weyl semimetallicity [23]. Moreover, the WTe_2 monolayer has been predicted to be a two-dimensional topological insulator [11] or a quantum spin Hall insulator [24], characterized by an insulating bulk and a conductive helical edge state. Unlike other TMDs, for which the 1*T* or 2*H* phase is the most stable structure [25–27], WTe_2 has an orthorhombic lattice structure (Td phase) in its ground state [28,29]. The Td phase has a relatively larger interlayer distance. Energetically the Td phase is 0.075 eV lower per formula unit of WTe_2 than the 2H phase [30,31]. For monolayer WTe_2, it is theoretically predicted [32–34] that the phase transition between the Td and 2H phases can be well controlled through external pressure, temperature or charge doping. Therefore, both Td and 2H phases need to be considered when searching for practical applications of WTe_2 nanomaterials. In their ground states, 2H-WTe_2 monolayer is a semiconductor, while Td-WTe_2 monolayer is a semimetal [25].

Previous studies demonstrate that reducing the dimensions of TMD materials can effectively change the electronic band structures around the Fermi surface. For example, WS_2, WSe_2, MoS_2 and $MoSe_2$ monolayers show indirect band gap electronic structures, while their bulk counterparts all contain direct band gaps [35,36]. In the present work, we try to study the electronic structure evolution when further reducing the dimension of a TMD into one-dimension. We take WTe_2 as an example for the TMD family because of the above mentioned interesting properties. Practically for design of future nanodevices, understanding of the physical parameters governing the electronic structures and thermo-

* Corresponding authors.
E-mail addresses: yang_yu@iapcm.ac.cn (Y. Yang), jyyan@bupt.edu.cn (J.-Y. Yan).

https://doi.org/10.1016/j.physleta.2018.06.031
0375-9601/

dynamic stabilities of WTe_2 nanoribbons is necessary. Presently WTe_2 monolayers have been regularly fabricated, but controlled fabrication of WTe_2 nanoribbons remains challenging. Theoretically, few theoretical studies on 2H-WTe_2 armchair nanoribbons can be traced, focusing on defect deformation [37] and tensile strain effects on transport characteristics [38].

In the present work, we carry out a first-principles study exploring the band gap dependence on the structural widths of WTe_2 nanoribbons, discussing the possibility of tailoring their electronic properties. Both the 2H and Td phases of monolayer WTe_2 are considered when building WTe_2 nanoribbons.

2. Calculation methods

All first-principles calculations are performed in the frame of density functional theory using the VASP code [39]. The exchange correlation is subjected to generalized gradient approximation in the Perdew–Burke–Ernzerhof form (PBE) [40,41]. The lattice constants as well as atomic coordinates are fully optimized until the residual forces are converged to be less than 0.01 eV/Å. The energy convergence criteria for self-consistent electronic optimizations is set to be 10^{-5} eV. The plane-wave basis had a cut-off energy of 400 eV. A $15 \times 15 \times 1$ k-point grid generated by using the Monkhorst method [42] is used for integrations over the Brillouin Zone. A vacuum layer larger than 20 Å is imposed both along the y and z directions (we define the x direction to be the periodic orientation) to avoid possible interactions between neighboring ribbons. Spin–orbit couplings are included in all calculations.

3. Results and discussion

Due to different symmetries, we design WTe_2 nanoribbons in different ways for the 2H and Td phases. The 2H-WTe_2 monolayer adopts a graphene-like symmetry. Thus we fabricate armchair and zigzag nanoribbons in the same way as that for graphene nanoribbons. The width number N is defined as the number of tungsten (W) atoms across the nanoribbon width. Different from 2H-WTe_2 monolayer, the Td-WTe_2 monolayer adopts a rectangular unit cell through formation of W chains along the y direction. Therefore, we fabricate nanoribbons of Td-WTe_2 monolayer by cutting it along the high-symmetry x and y directions, which are denoted as Tdx and Tdy nanoribbons. In the same way, we define the width number N as the number of W atoms across the nanoribbon width.

The optimized atomic structures of WTe_2 monolayers and nanoribbons are depicted in Fig. 1. After geometry optimizations, we find that the atomic structures of 2H- and Td-WTe_2 monolayers are almost the same as that in their bulk counterparts. We list our calculated lattice constants and electronic band gaps of WTe_2 monolayers in Table 1, together with previous experimental [43] and theoretical results [44–46]. One can see that our results are in good agreements with previous reports. When cutting WTe_2 monolayers into one-dimensional nanoribbons, large structural relaxations can be found at the nanoribbon edges. For the zigzag and Tdy WTe_2 nanoribbons, we have to add additional Te atoms to saturate the dangling bonds of edge W atoms, so that the geometry optimizations converge. The optimized zigzag and Tdy WTe_2 nanoribbons are structurally depicted in Figs. 1(d) and 1(f). One can see that the edges are quite stable with the edge atoms undergoing negligible atomic movements during geometry optimizations. In comparisons, although the stoichiometric armchair and Tdx WTe_2 nanoribbons converge during geometry optimizations, large atom redistributions can be found at their edges. Fig. 1(c) shows a typical edge structure for armchair WTe_2 nanoribbon (with the width number of $N = 8$). As shown, the outermost edge

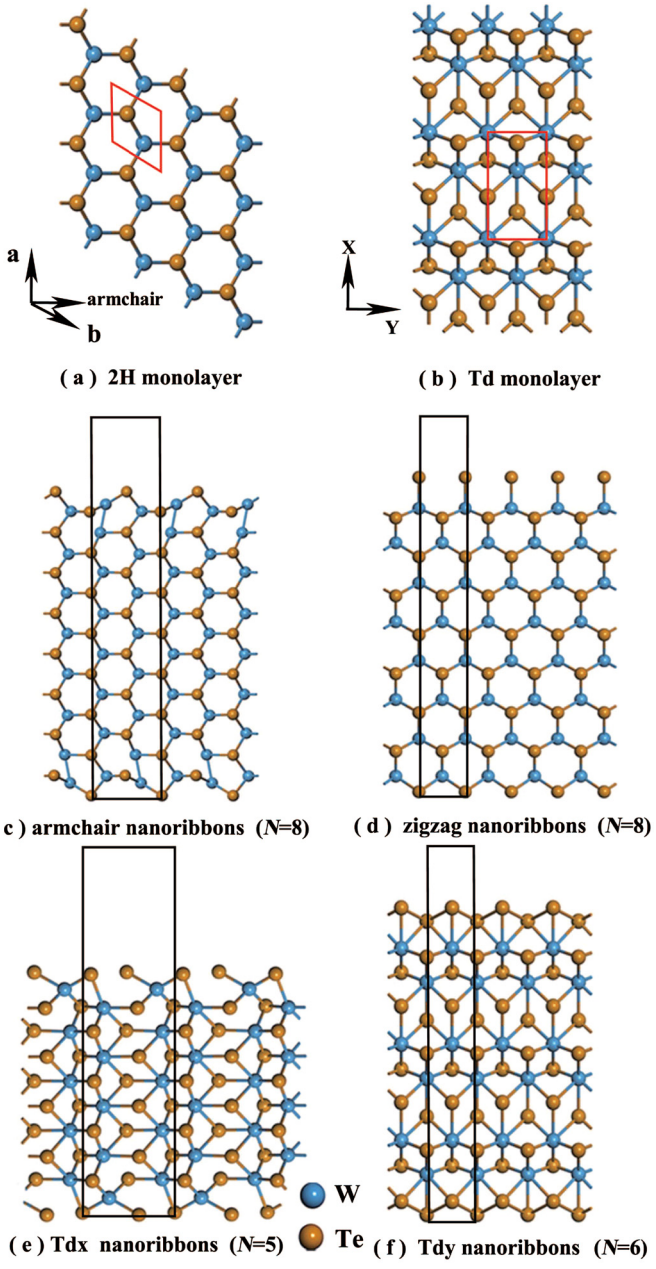

Fig. 1. (Color online.) Optimized structures of WTe_2 monolayers and nanoribbons. (a) and (b) The monolayer structures of 2H- and Td-WTe_2, with their unit cells indicated by red lines. (c) and (d) Armchair and zigzag nanoribbons cut from 2H-WTe_2 monolayer. (e) and (f) Tdx and Tdy nanoribbons cut from Td-WTe_2 monolayer. The black quadrilaterals depict corresponding unit cells for each nanoribbons.

W atom tends to bond with a next outermost W atom, and subsequently two arc structures form at the two edges of the armchair WTe_2 nanoribbon. The bond length of armchair boundary altered significantly to 2.768 Å, 2.694 Å, which 2.730 Å in plane. A typical structure for Tdx WTe_2 nanoribbons is shown in Fig. 1(e). Structurally, the edge W atoms tend to be surrounded by 4 tellurium (Te) atoms occupying the tetrahedral center position. While in the center area of the nanoribbon, each W atom is surrounded by 6 Te atoms that form an octahedron. The large edge relaxations indicate that W atoms cannot solely act as edge atoms.

We then perform systematic electronic structure calculations for different types of WTe_2 monolayers and nanoribbons. Fig. 2 shows the typical electronic band structures for 2H-WTe_2 monolayer and nanoribbons. As shown, 2H-WTe_2 monolayer is a direct

Please cite this article in press as: J.-H. Wang et al., First-principles predictions of the geometries and electronic structures of tungsten ditelluride nanoribbons, Phys. Lett. A (2018), https://doi.org/10.1016/j.physleta.2018.06.031